Response to Referee #1 (acp-2022-729)

We Thank Reviewer for his/her constructive comments

Responses to the Specific comments

General comments: This work estimated multiple emissions using the EnKF with the state augmentation method during the COVID-19 pandemic. Then, they assessed the unbalanced emission reduction of different species during the restriction. The manuscript is well organized and contains detailed analysis. However, the authors have some issues to be clarified in the manuscript for the final publication in ACP.

Reply: The authors appreciate the reviewer for his/her constructive and up-to-point comments. We have carefully considered the comments and revised the manuscript accordingly. Please refer to our responses for more details given below.

Comment 1: Line 91 & 285 (Weak motivation): The EnKF coupled with the state augmentation used in this study could be a more advanced method than inversed single estimation (Zhang et al., 2020; 2021, Feng et al., 2020, & Hu et al., 2022) in terms of emission estimation for multiple species. However, it could be less cost-effective. Also, as mentioned in the manuscript (line 285), it shows a similar performance with the single estimation of SO_2 (Hu et al., 2022). In other words, the inversed single estimation can be better, considering both performance and computational cost. Therefore, considering these issues, the authors need some more explanation or justify the use of your method to enhance the motivation for this work.

Reply: Thanks for this suggestion. The EnKF coupled with the state augmentation is a commonly used method for the estimations of multi-species' emissions (Miyazaki et al., 2017; Ma et al., 2019; Peng et al., 2018). In this method, the emissions of different species are simultaneously estimated by including them as a part of the state vector together with the chemical concentrations using the ensemble model simulations and observations. The mass balanced method used in Zhang et al. (2020) and Zhang et al. (2021) is to adjust the model emissions based on the modeled local ratio between concentrations and emissions. Although it has lower computational cost than the EnKF method since it does not need to run an ensemble of model simulation, it has difficulties in accounting for the nonlinear relationship between the concentrations and emissions, thus is more commonly used in the inversions of short-lived species (e.g., NO_x) under relatively coarse (>1°) resolution (Streets et al., 2013). The EnKF method instead can consider the nonlinear relationship between the emissions and concentrations (as we illustrated in our response to comment 2), and can be used for longer-lived species (e.g., SO_2, $PM_{2.5}$ and CO) at finer model

resolutions (Streets et al., 2013). The four-dimensional variational assimilation (4DVar) method used in Hu et al. (2022) is an advanced inversion method similar to the EnKF method, and they have different strengths and weakness (Skachko et al., 2014). The 4DVar uses an adjoint model of a chemical transport model (CTM) to estimate the emissions, thus it requires the development and maintenance of an adjoint model, which is technically difficult and cumbersome for the complex CTM. The EnKF method does not require an adjoint model and is easily implemented. Besides, although 4DVar does not need to run an ensemble of simulation, it needs to solve a complex optimization problems for a large chemical model system, therefore, the 4DVar have comparable computational costs with the EnKF method (Skachko et al., 2014). Similar to our method, Feng et al. (2020) used the EnKF method to estimate the emission changes of NO_x during COVID-19 pandemic, but they did not constrain the emissions of other species. Due to the chemical reactions in the atmosphere, the concentrations of different species are interrelated with each other. For example, the ambient $PM_{2.5}$ is not only primarily emitted, a large portion of them is also formed secondarily through reactions with several gaseous precursors, such as NO_2 and SO_2. This means that inversed single estimation may cause biases in the inversed $PM_{2.5}$ emission if the errors in emissions of NO_2 and SO_2 were not corrected synchronously. Assimilations of CO measurement also influences the inversion of NO_2 emission due to its influence on the OH concentration in the atmosphere (Miyazaki and Eskes, 2013). Therefore, doing the multi-species inversion estimation can provide more constraints on the atmospheric chemical system than the inversed single estimation and thus can produce more reasonable inversion results (Miyazaki and Eskes, 2013; Peng et al., 2018). The inversion estimation for SO_2 may be less affected by assimilations of other species due to its less dependence on other species. As a result, our inversion results showed a similar performance with the single estimation of SO_2 in Hu et al. (2022). Besides, the emissions of different species were perturbed simultaneously in our method, thus the ensemble simulation only needs to be performed once. The computational cost only increased slightly in the analysis step. Therefore, the multi-species' inversion method used in our study has its strength over the inversed single estimation method used in previous studies. Following the suggestions of reviewers, we give more explanation for the use of our method in the revised manuscript (please see lines 161–178)

Comment 2: Line 126: The authors need to clarify how to consider the non-linearity between NOx emission (for estimation) and NO_2 concentration (of observation). Additionally, in-situ NO_2 observation may be based on the commercial chemiluminescent instrument. While the instrument system converts NO_2 to NO through a molybdenum converter, other species, such as peroxyacetyl nitrates (PANs) and

HNO3, are also simultaneously converted to NO. The other species account for a large portion of the converted NO molecules. For example, Dunlea et al. (2007) showed the interference in the chemiluminescence detection accounting for up to 50% of ambient NO_2. In other words, the observed NO_2 is almost equivalent to ambient NO_y. Also, PAN is thermally sensitive (and it is also related to the temperature shown in Figure 10). The rapid decrease in NO_x emission is strongly linked to this issue. Therefore, the authors also need to explain how to treat these issues in your calculation.

Reply: Thanks for this important comment. In EnKF method, the relationship between the concentrations and emissions of related species was determined by the background error correlations, which is estimated from the ensemble model simulations. Since the chemistry transport model used in our study is a nonlinear model which considers the physical and chemical processes in the atmosphere, the ensemble simulation is able to represent the nonlinear evolution of the error correlations. This allows the nonlinear relationships between NO_2 concentrations and NO_x emissions to being considered through the use of background error covariance produced by ensemble simulations (Evensen, 2009; Miyazaki et al., 2012). Following the suggestions of reviewer, we have clarified this in the revised manuscript (please see lines 165–167).

As the reviewer mentioned, the NO_2 measurement made by CNEMC is based on the chemiluminescent analyser with a molybdenum converter. We agree with the reviewer that the interference of HNO_3, PAN and alkyl nitrates (AN) can lead to an overestimation of NO_2 (Dunlea et al., 2007; Lamsal et al., 2008) and may lead to spurious decreases of NO_x emissions. Due to the lack of synchronous observations of HNO_3, PAN and AN, it is hard to directly correct such overestimations in the NO_2 measurements. Previous studies (Cooper et al., 2020; He et al., 2022) usually use chemical transport model to simulate NO_x, HNO_3, PAN and AN to produce correction factors (CFs) for the NO_2 measurements using the following relationship proposed by Lamsal et al. (2008):

$$CF = \frac{[NO_2]}{[NO_2]+0.95[PAN]+0.35[HNO_3]+\sum[AN]} \quad \text{(R1)}$$

but the calculation of CF could be affected by the simulation errors in the model caused by uncertainties in emission inventory or other error sources, which may contaminate the observations. Therefore, similar to Feng et al. (2020), we did not correct the NO_2 measurement in our inversion of NO_x emissions since there were large uncertainties in the NO_x emissions during the COVID-19 pandemic that possibly led to erroneous CF. Instead, the EnKF is capable of considering the errors in the observations during the assimilation through the use of observation error covariance matrix. The interference in the chemiluminescence detection to the NO_2 measurement was thus treated as a kind of observation error in

our study. According to our estimates, the total observation error of NO_2 measurements was about 6–10 $\mu g/m^3$. To investigate whether our settings of observation error can fully cover the errors induced by the chemiluminescence monitor interference, we calculated the CF according to Eq. (R1) based on the simulated NO_2, HNO_3, PAN and AN using the inversed emission inventory to alleviate the effects of emission uncertainty on the CF calculations. Figure R1 shows the calculated CFs for NO_2 measurements over different regions of China during COVID-19 pandemic, which generally ranged from 0.75 to 0.99. The CF values over NCP, NE, NW and Central were generally stable throughout the COVID-19 pandemic, all larger than 0.9, suggesting that chemiluminescence monitor interference only has slight effects on the NO_2 measurement. Over the SE and SW regions, there was a drop of CF values during the lockdown period, followed by an increase after the lockdown. This indicates that the decline of NO_2 concentrations during lockdown period may be larger in these two regions.

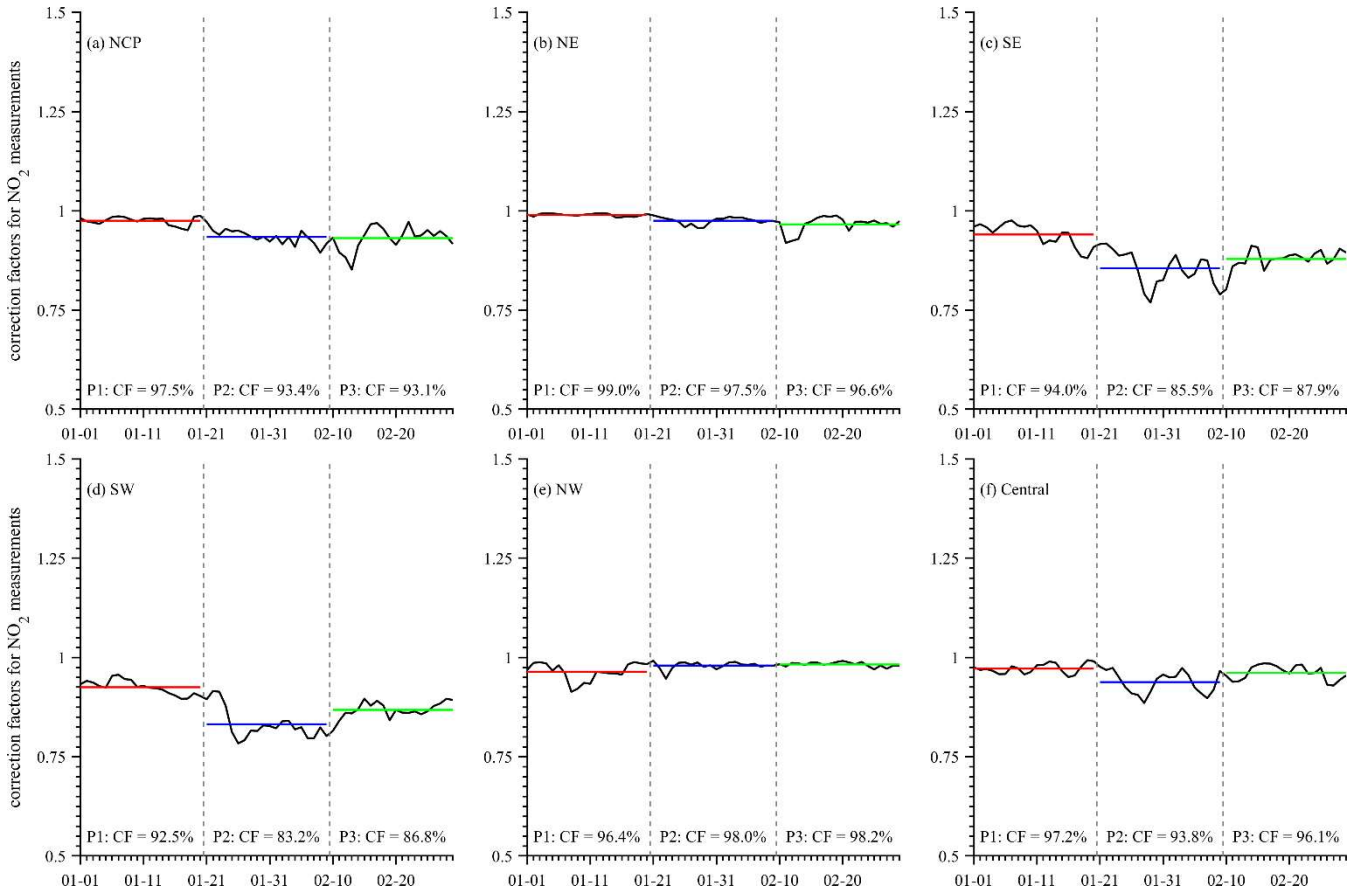

Figure R1: Time series of calculated CFs for NO_2 measurements over (a) NCP, (b) NE, (c) SE, (d) SW, (e) NW and (f) Central region during COVID-19 pandemic. The averaged CF values during different stages of COVID-19 pandemic are also labeled.

As shown in Figure R2, the overestimations were generally lower than 3 $\mu g/m^3$ over different regions of China throughout the COVID-19 pandemic, which is smaller than the observation errors we assigned in the assimilation, suggesting that the observation error caused by the chemiluminescence monitor interference were contained in the assimilation. In order to quantify the influences of chemiluminescence monitor interference on the inversed NO_x emission, an additional inversion

experiment was conducted based on the corrected NO_2 measurement using the calculated CF. The results suggest the chemiluminescence monitor interference in the NO_2 observations had weak impacts on the inversed NO_x emissions as seen in Fig. R3 and Fig. R4, which display the comparisons of the inversed NO_x emission with and without correction in respect of the magnitude and change ratio during different stage of COVID-19 pandemic. The differences in the magnitude of inversed NO_x emissions caused by correction were about 2–7% over the NCP, NE, NW and Central, and were about 10–13% over the SE and SW. Differences in the emission reductions of NO_x were also small, which was about 0.3 to 4.1 percentage points. Consistent with the reviewer, the result suggests that the chemiluminescence monitor interference is a potential factor that influence the inversion of NOx emission, which is a limitation of current work. However, it might not significantly influence our inversion results and the main conclusions. Considering this, we added a discussion about the effects of chemiluminescence monitor interference to inform the potential reader in the revised manuscript (please see lines 143–158) and supplement (please see lines 15–39 and Figure S16–S19).

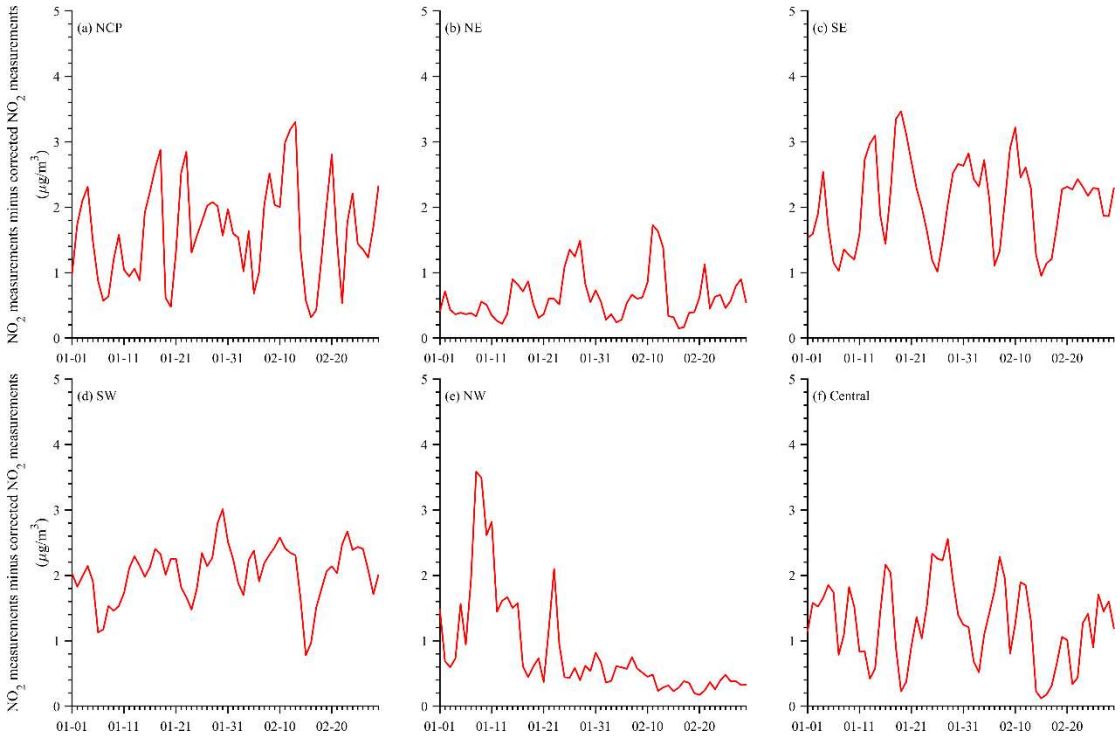

Figure R2: the difference of NO_2 measurement before and after the corrections of chemiluminescence monitor interference over (a) NCP, (b) NE, (c) SE, (d) SW, (e) NW and (f) Central during the COVID-19 period.

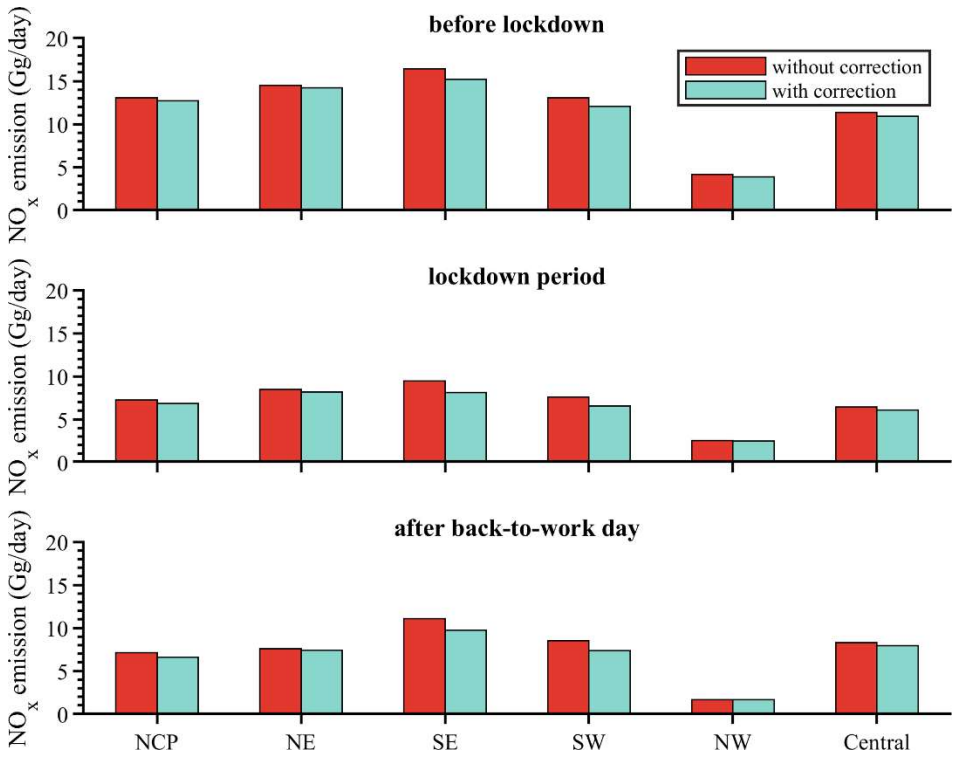

Figure R3 Comparisons of inversed NO_x emissions with (blue) and without (red) correction of NO_2 measurement over different regions of China during different period of COVID-19 pandemic.

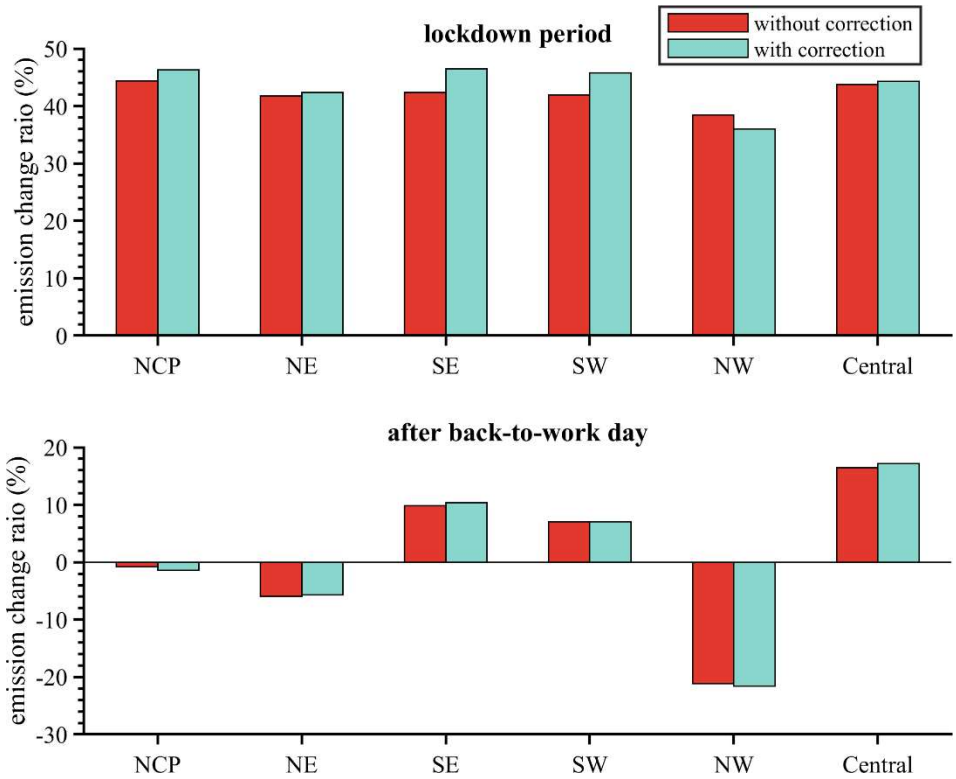

Figure R4 Comparisons of the calculated emission change of NO_x emissions based on the inversion results with (blue) and without (red) correction of NO_2 measurement over different regions of China.

Comment 3: Line 90: Levelt et al. (2022) is not related to the emission inversion technique. The authors had better discard this paper in the manuscript.

Reply: We feel sorry for this inappropriate citation. We have removed this paper in the revised manuscript.

Comment 4: Line 105: Anthropogenic and other emission inventories used in the simulations during the COVID-19 pandemic are based on 2010 or relatively long ago. These emission rates could be significantly higher than those during the COVID-19 pandemic. The higher emission rates are significantly related to the concentration of atmospheric species like O_3. Therefore, the authors need to justify the uses of such emission inventories in the simulations

Reply: Thanks for this important comment. We agree with the reviewer that a prior emission inventory used in our study is significantly higher than those during the COVID-19 pandemic due to the restrict emission control policy over the past decades. However, due to the lack of updated activity data and emission factors, the latest bottom-up anthropogenic emission inventory in China that were available is for the base year 2018, which could be also higher than those during COVID-19 pandemic. Considering this, we have developed the iteration emission inversion technique to address this issue. According to the inversion results, the iteration emission inversion significantly reduced the large biases in the a priori emission inventory and is able to reproduce the emission levels during the COVID-19 pandemic. Therefore, we did not update the a priori emission inventory to more recent emission inventory during the assimilation.

To test the influences of the choice of a priori emission inventory on the inversion estimation, a new inversion run was conducted based on the a priori emission inventory for base year 2018. This new emission inventory is comprised of the anthropogenic emissions obtained from HTAPv3 (Crippa et al., 2023), the biogenic, soil and oceanic emissions obtained from the CAMS global emission inventory (https://ads.atmosphere.copernicus.eu/cdsapp#!/dataset/cams-global-emission-inventories?tab=overview, last access: March 15, 2023) and biomass burning emissions obtained from the Global Fire Assimilation System (GFAS)(Kaiser et al., 2012). The detailed steps of the new inversion estimation were same as those elucidated in Sect.2. Figure R5–7 show the comparisons of inversion results based on the a priori emissions for base 2010 with those based on the a priori emissions for 2018. The results suggest that the inversion results based on the 2010 and 2018 inventory were broadly close to each other, while the inversion results based on 2018 inventory were relatively higher than those based on 2010 inventory, reflecting the uncertainty in our inversion results caused by the choice of the a priori emission inventory. Figure R8 and R9 show the temporal variations of the multi-species' emissions during COVID-19 pandemic at the national and regional scales derived from the inversion results based on 2018 inventory, which consistently showed that the NO_x emissions decreased much larger than other species. In all, the sensitivity experiment demonstrates that the choice of a priori emission inventory may not obviously

influence the main conclusion of our study, but can lead to uncertainty in the magnitude of the inversion results which is a limitation of current work. Therefore, a discussion about the influence of a priori emission inventory has been added to the revised manuscript (please see lines 492–505) and supplement (please see Figure S20–S24) to inform the potential readers.

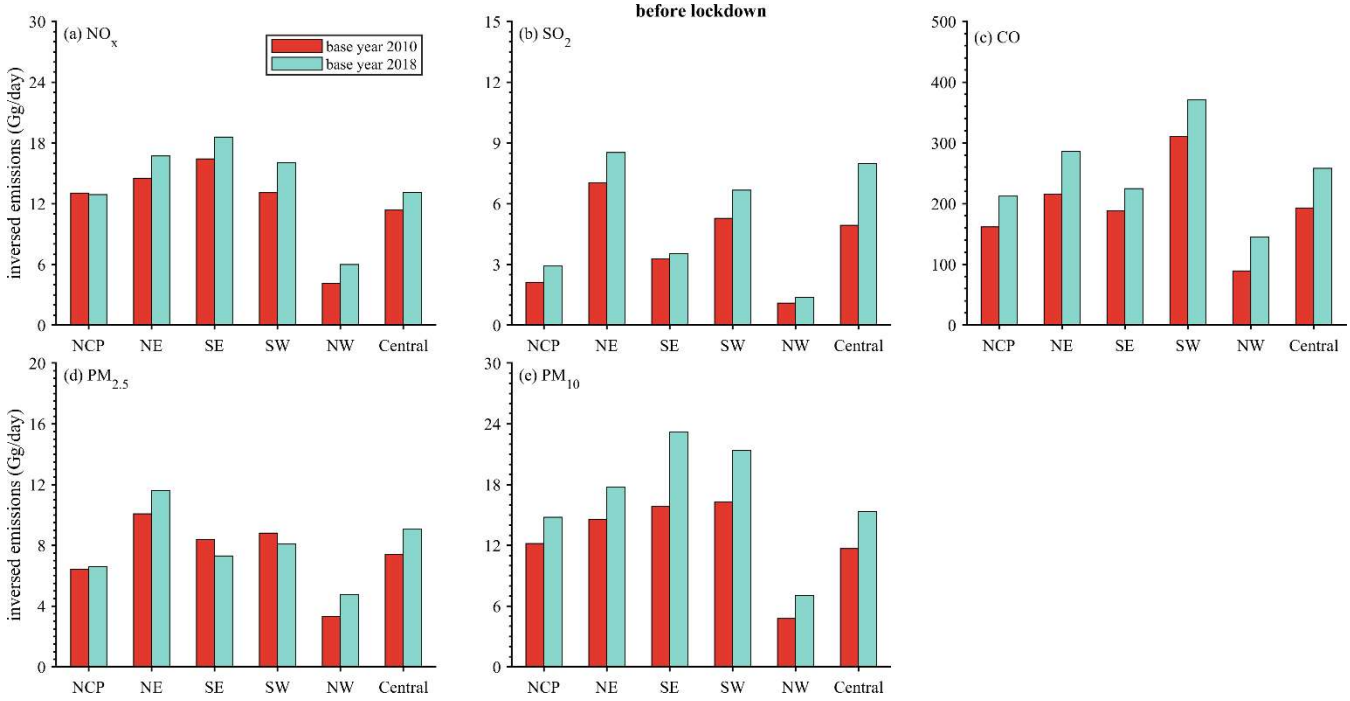

Figure R5: Comparisons of the inversion estimated total emissions of (a) NO_x, (b) SO_2, (c) CO, (d) $PM_{2.5}$ and (e) PM_{10} before lockdown using the a priori emission inventory for base year 2010 (read) with those using the a priori emission inventory for base 2018 (blue).

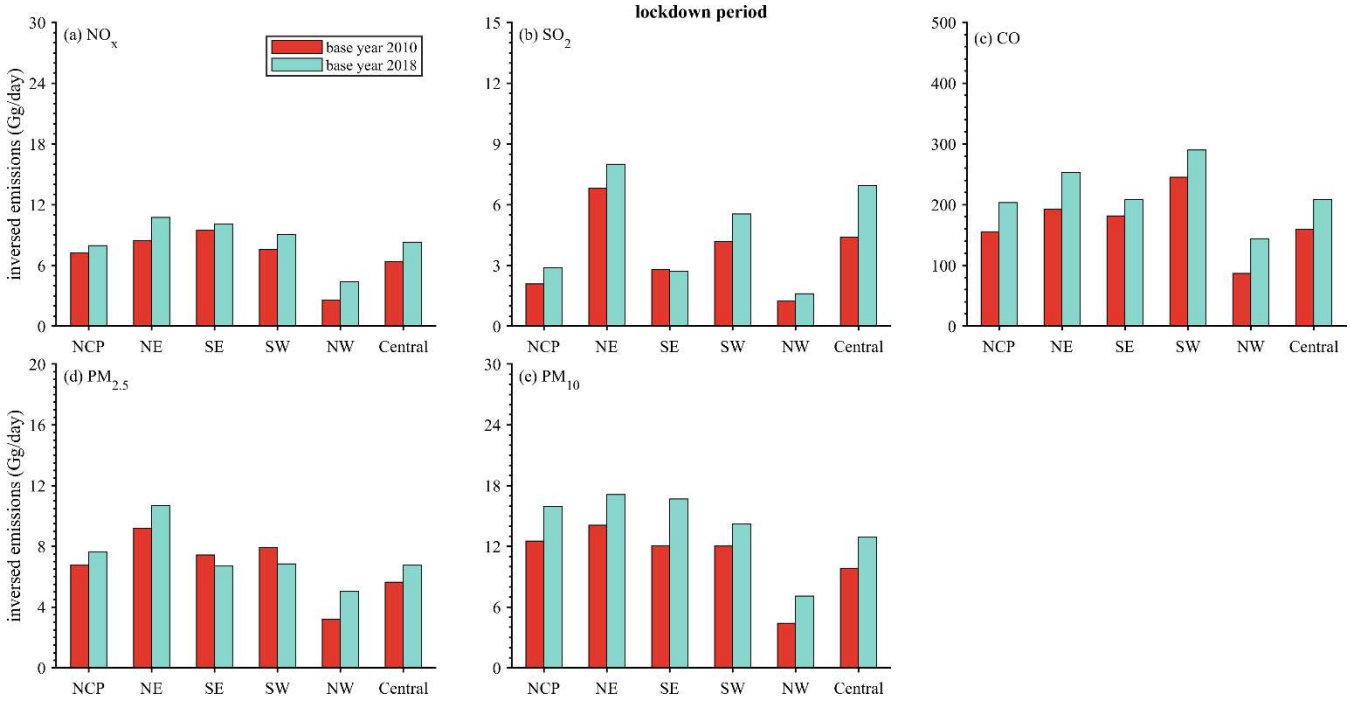

Figure R6: Same as Fig.R5 but for the p2 period (lockdown period).

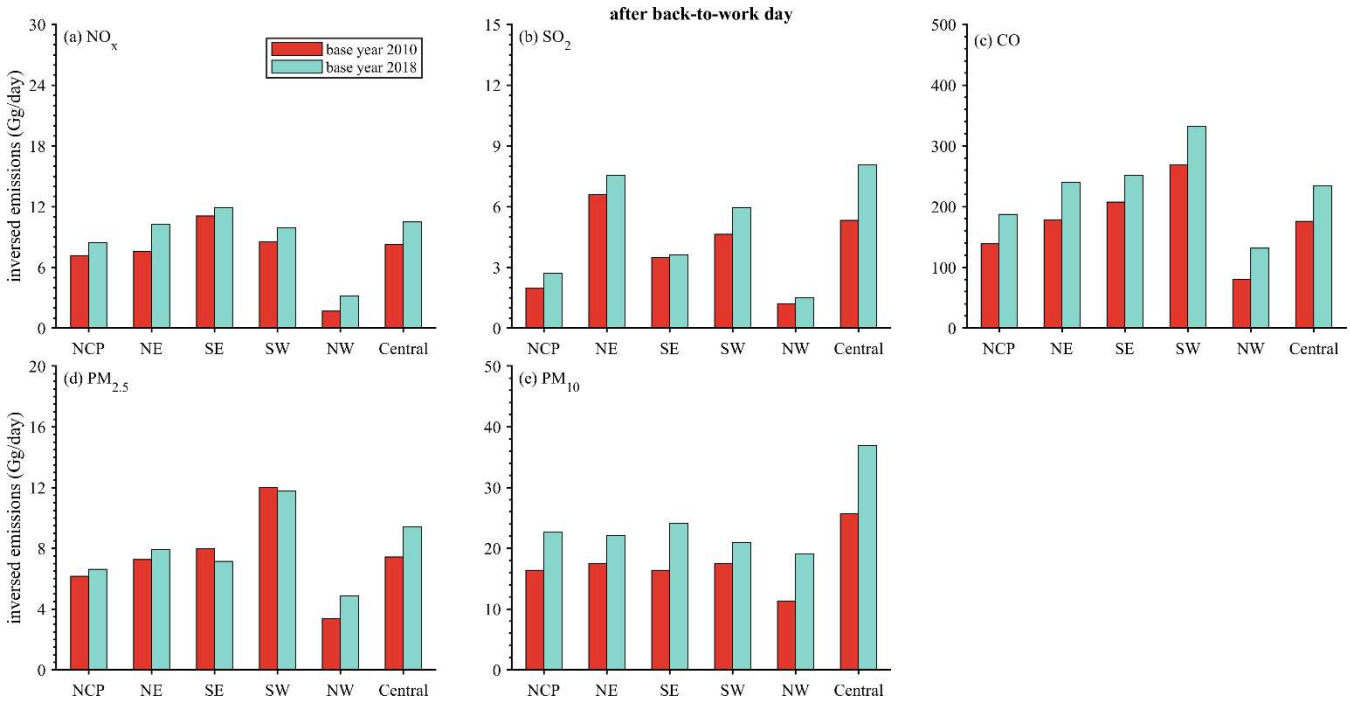

Figure R7: Same as Fig. R5 but for the P3 period (after back-to-work day).

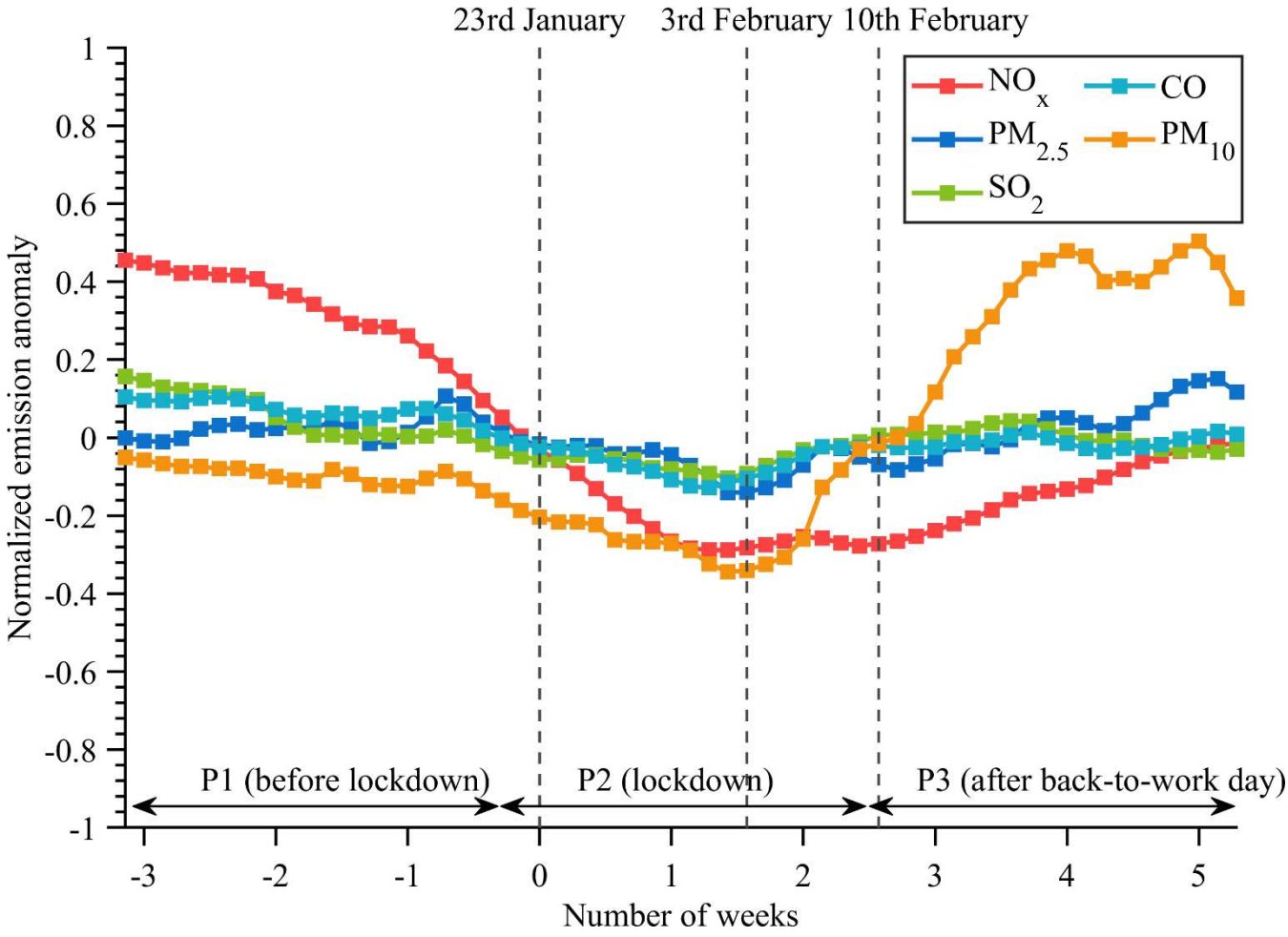

Figure R8: Time series of normalized emission anomalies estimated by inversion results for different species in China from 1st January to 29th February 2020 using the a priori emission inventory for 2018.

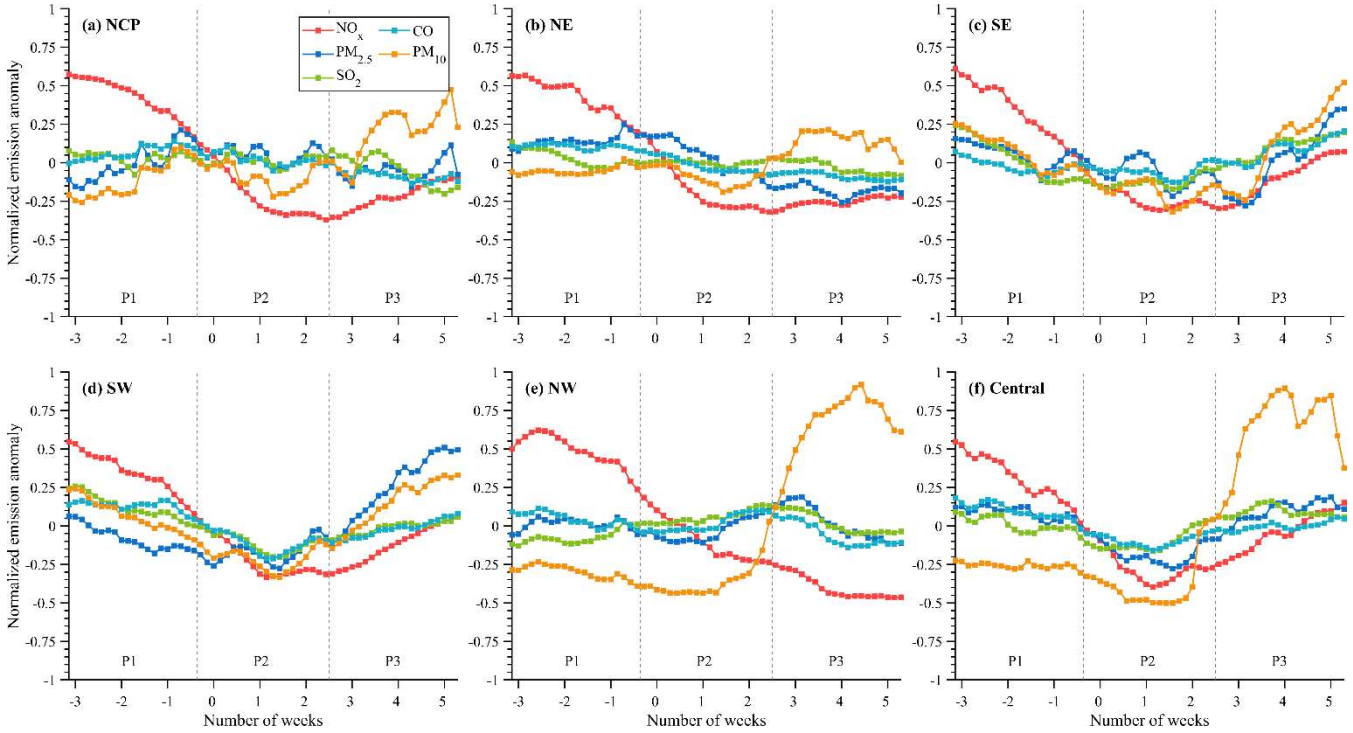

Figure R9: Time series of normalized emission anomalies estimated by inversion results for different species over (a) NCP region, (b) NE region, (c) SE region, (d) SW region, (e) NW region and (f) Central region from 1st January to 29th February 2020 using the a priori emissions for 2018.

Comment 5: Line 138: The explanation of EI and MI (from both MET and EMIS change scenarios) is rather complicated. The authors need to clarify it. Tabulating or illustrating the scenarios or cases makes it easier for the readers to understand them.

Reply: Thanks for this suggestion. We have added two tables in the revised manuscript to illustrate the different scenarios and the meaning of different items in the calculation of EI and MI (please see Table 2 and Table 3 in the revised manuscript):

Table R1 configuration of simulation scenarios

Scenarios	Meteorology input	Emission input	Purpose
BASE scenario	varied meteorological condition from pre lockdown to lockdown period	varied emission from pre-lockdown to lockdown period	To estimate the total changes of air pollutant concentrations induced by emission and meteorological change
MET change scenario	varied meteorological condition from pre-lockdown to lockdown period	constant emissions during pre-lockdown and lockdown period	To estimate the impacts of meteorological changes on the air pollutants
EMIS change scenario	constant meteorological during pre-lockdown and lockdown period	varied emission from pre-lockdown to lockdown period	To estimate the impacts of emission changes on the air pollutants

Table R2 descriptions of different items used in the calculation of meteorological-induced and emission-induced changes of air pollutant concentrations

notation	Description
MI	meteorological-induced changes of air pollutant concentrations
EI	emission-induced changes of air pollutant concentrations
$MI_{MET\ change\ scenario}$	meteorological-induced changes of air pollutant concentrations calculated by the MET change scenario
$EI_{MET\ change\ scenario}$	emission-induced changes of air pollutant concentrations calculated by total changes minus $MI_{MET\ change\ scenario}$
$EI_{EMIS\ change\ scenario}$	emission-induced changes of air pollutant concentrations calculated by the EMIS change scenario
$MI_{EMIS\ change\ scenario}$	meteorological-induced changes of air pollutant concentrations calculated by total changes minus $EI_{EMIS\ change\ scenario}$
$conc_{p1,BASE\ scenario}$	averaged concentrations of air pollutants during P1 period under the BASE scenario
$conc_{p2,BASE\ scenario}$	averaged concentrations of air pollutants during P2 period under the BASE scenario
$conc_{p1,MET\ change\ scenario}$	averaged concentrations of air pollutants during P1 period (pre-lockdown) under the MET change scenario
$conc_{p2,MET\ change\ scenario}$	averaged concentrations of air pollutants during P2 period (lockdown) under the MET change scenario
$conc_{p1,EMIS\ change\ scenario}$	averaged concentrations of air pollutants during P1 period under the EMIS change scenario
$conc_{p2,EMIS\ change\ scenario}$	averaged concentrations of air pollutants during P2 period under the EMIS change scenario
$contri_{met}$	relative contributions (%) of the meteorological variations to the changes in air pollutant concentrations
$contri_{emis}$	relative contributions (%) of the emission changes to the changes in air pollutant concentrations

Comment 6: Line 218: The authors need to define P1, P2, and P3 on Line 218, not on Line 247. Also, the authors need to add some lines for P1, P2, and P3 on the x-axis of Figure 4.

Reply: Thank you so much for your careful check. We have changed the position where the P1, P2 and P3 were defined in the revised manuscript (please see lines 104–106) and some lines for P1, P2 and P3 were also added on the x-axis of Figure 4 and Figure 5.

Comment 7: Line 268: The performance in the O_3 simulation is relatively poor. As mentioned in the manuscript, the lower performance is related to VOC emission. Since the VOC emission used in the simulations is made for 2010, there are some time gaps. Therefore, the authors need to compare the VOC emission rates with the recent or 2019 database and then make an additional explanation of (expected) ozone concentrations.

Reply: Thanks for this comment. Following the suggestions of reviewer, we have compared the NMVOC emissions for base year 2010 with the NOVOC emissions for base year 2018. To prevent the inconsistency between different inventory, the anthropogenic part of NMVOC emissions were obtained from the HTAP_v3 inventory(Crippa et al., 2023), which is an updated version of the anthropogenic emission inventory (HTAP_v2.2) we used in our study. The biogenic part was obtained from the CAMS biogenic emissions calculated using the Model of Emissions of Gases and Aerosols from Nature (MEGAN) driven by ERA-Interim meteorological fields (Granier, C. et al., 2019). The NMVOC emissions from wildfires and biomass burning was obtained from the Global Fire Assimilation System (GFAS)(Kaiser et al., 2012). Figure R5 shows the comparisons of NMVOC emissions for base year 2010 with those for base year 2018 over different regions of China. It shows that the NMVOC emissions for base year 2010 were generally lower than those for 2018 except over the SW regions. Considering the increasing trend of NMVOC emissions in China (Li et al., 2019), the underestimates of NMVOC emissions for base year 2020 due to the use of old emission inventory may be larger. This is in line with the negative biases in the simulated O_3 concentrations over these regions. Following the suggestion of reviewer, we have clarified it in the revised manuscript (please see lines 294–297).

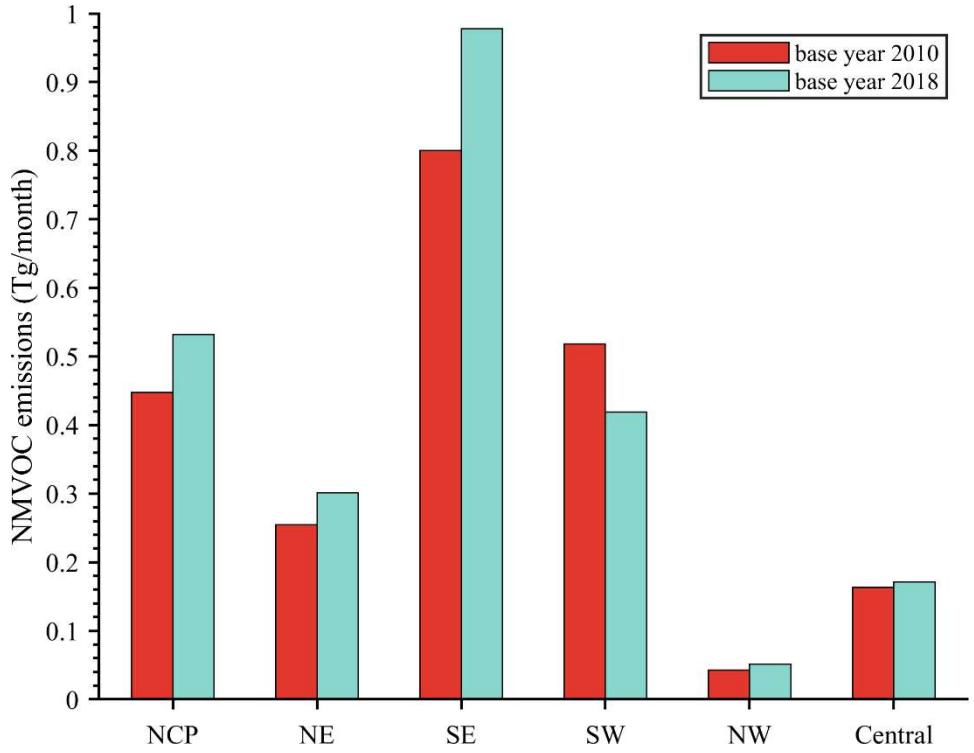

Figure R5 comparisons of the NMVOC emissions for base year 2010 with those for 2018 over different regions of China.

Comment 8: Line 289 & 303 – 304: The authors need to explain what causes increases in PM_{10} during the P3 in Figure 4, Figure 5e, and 5f. The authors explained these are related to the sandstorm. However, the concentration of PM_{10} during the P3 period was rather low in the NW and Central regions.

Reply: Thanks for this suggestion. The $PM_{2.5}/PM_{10}$ ratio was used to investigate the causes of the increases in PM_{10} emission in the revised manuscript, which is an indicator of the potential sources of particular matter. A lower $PM_{2.5}/PM_{10}$ ratio usually indicates significant contributions from natural sources such as dust (Wang et al., 2015; Fan et al., 2021). As we can see from Fig.R6, the $PM_{2.5}/PM_{10}$ ratio was stable during the P1 and P2 period, but it decreased substantially during the P3 period, from 0.81 to 0.48 over the NW region and from 0.77 to 0.53 over the Central region, which suggests larger contributions of dust emissions to the PM10 concentrations during the P3 period. Moreover, the NW and Central region are typical source areas of dust in China, therefore the increasing of PM_{10} emissions over NW and Central regions may be mainly related to the enhanced dust emissions. following the suggestion of reviewer, we added more explanations to the increased PM_{10} emissions over the NW and Central region in the revised manuscript (please see lines 342–348).

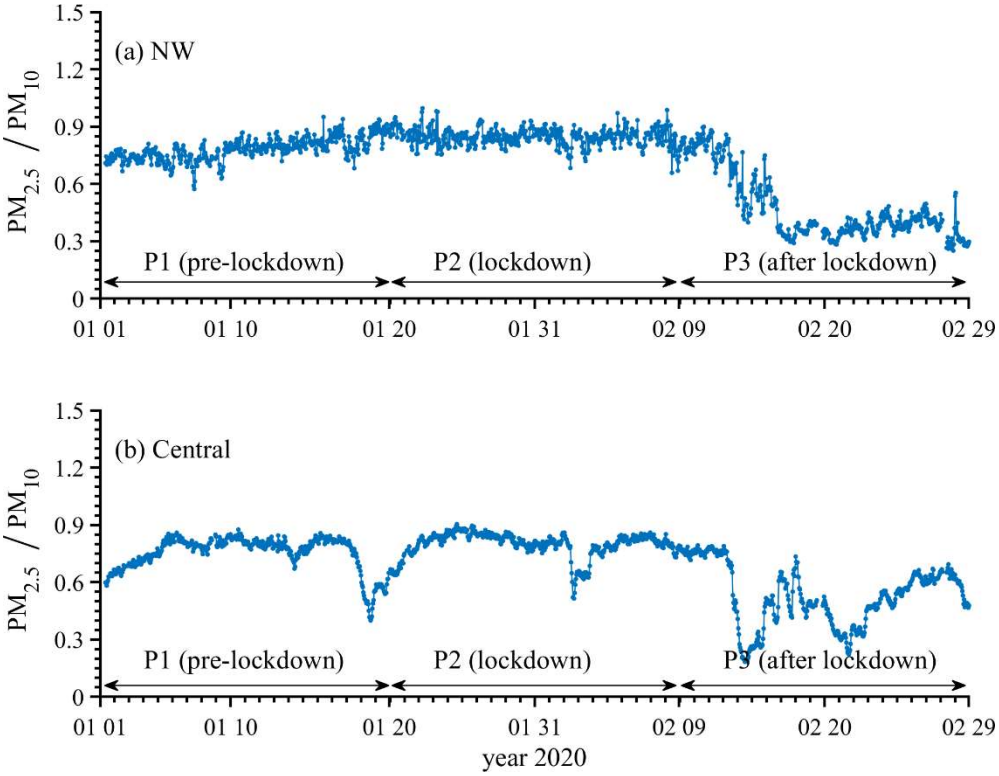

Figure R6 timeseries of $PM_{2.5}/PM_{10}$ ratio during COVID-19 pandemic over (a) NW and (b) Central region

Comment 9: Line 295: The explanation is not sufficient for the $PM_{2.5}$ emission increase in the NCP region. The observation done by Dai et al. (2020) was carried out at a single site in Tianjin.

Reply: Thanks for this important comment. We conducted a more detailed analysis on the possible causes of the $PM_{2.5}$ emission increases in the NCP region through literature review and analysis of the $PM_{2.5}$ compositions. Previous researches suggested that the increases of $PM_{2.5}$ emissions over the NCP region may be due to the increased emissions from industry and fireworks (Dai et al., 2020; Li et al., 2021; Ma et al., 2022; Zuo et al., 2022). Based on the measurement of stable Cu and Si isotopic signature and distinctive metal ratios in Beijing and Hebei, Zuo et al. (2022) analyzed the variations in the $PM_{2.5}$ sources in Beijing and Hebei during the COVID-19 pandemic, which provides evidences that the primary $PM_{2.5}$ emissions did not decrease in Beijing and Hebei, and that the PM-associated industrial emissions may instead increase during the lockdown period. The increased industrial heat sources detected by Li et al. (2022) based on VIIRS active fire data also supported the increased industrial emissions over the NCP region during lockdown period. Figure R7 shows the variations of the concentrations of potassium (K^+) and magnesium (Mg^{2+}) ion, two important fingerprints of the firework emissions, over the NCP region during COVID-19 pandemic. Measurement of K^+ and Mg^{2+} over the NCP region were obtained from China National Environmental Monitoring Center (CNEMC) with site distribution shown in Fig. 11. Substantial increases of K^+ and Mg^{2+} concentrations could be observed during the Spring Festival over

the NCP region, which indicates larger contributions of firework emissions to the $PM_{2.5}$ concentrations during the lockdown period. this is consistent with the field measurements in Beijing and Tianjin conducted by Ma et al. (2022) and Dai et al. (2020). These results suggested that the increased industrial $PM_{2.5}$ emissions, together with firework emissions may contribute to the increased $PM_{2.5}$ emissions over NCP region, which compensated the emission reductions from the traffic emissions. Based on this analysis, we have added more detailed discussions about the possible reason for the increases of $PM_{2.5}$ emissions over the NCP region in the revised manuscript (please see lines 322–333) and supplement (please see Figure S15).

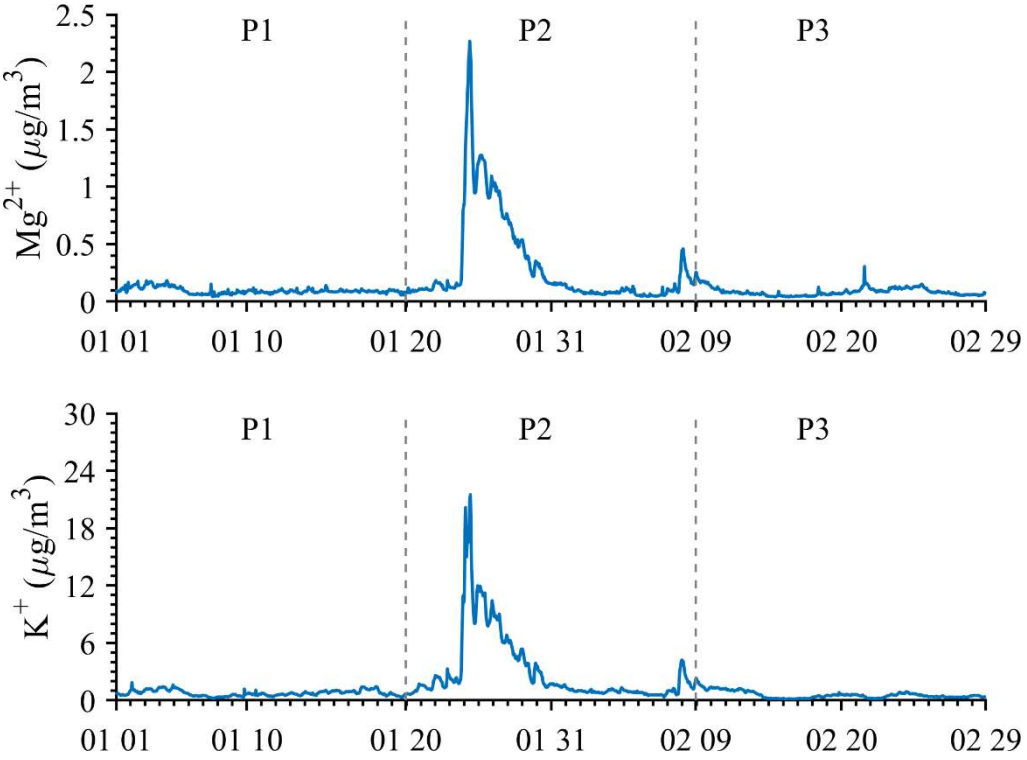

Figure R7: Timeseries of averaged concentrations of potassium and magnesium ion during COVID-19 pandemic over the NCP region.

Comment 10: Line 340: The authors also need to mention that the O_3 is under-simulated in all regions (refer to Figure S6).

Reply: Thanks for this comment. The underestimations of the O_3 have been pointed out in the revised manuscript (please see lines 389).

Minor comments:

Comment 11: Line 32: measurement -- > measure or measures

Reply: Done.

Comment 12: Line 33: remove 'both'.

Reply: Done.

Comment 13: Line 261. It is probably Table S1, not Table S4

Reply: Done.

Comment 13: Lines 277 and 280: The authors need to confirm the numbers in these lines (and Table 2).

Reply: Thanks a lot for your careful check. We have corrected the wrong number in lines 277 and 280. Please see lines 305 and 308 in the revised manuscript.

References

Cooper, M. J., Martin, R. V., McLinden, C. A., and Brook, J. R.: Inferring ground-level nitrogen dioxide concentrations at fine spatial resolution applied to the TROPOMI satellite instrument, Environ. Res. Lett., 15, 12, https://doi.org/10.1088/1748-9326/aba3a5, 2020.

Crippa, M., Guizzardi, D., Butler, T., Keating, T., Wu, R., Kaminski, J., Kuenen, J., Kurokawa, J., Chatani, S., Morikawa, T., Pouliot, G., Racine, J., Moran, M. D., Klimont, Z., Manseau, P. M., Mashayekhi, R., Henderson, B. H., Smith, S. J., Suchyta, H., Muntean, M., Solazzo, E., Banja, M., Schaaf, E., Pagani, F., Woo, J. H., Kim, J., Monforti-Ferrario, F., Pisoni, E., Zhang, J., Niemi, D., Sassi, M., Ansari, T., and Foley, K.: HTAP_v3 emission mosaic: a global effort to tackle air quality issues by quantifying global anthropogenic air pollutant sources, Earth Syst. Sci. Data Discuss., 2023, 1-34, https://doi.org/10.5194/essd-2022-442, 2023.

Dai, Q., Liu, B., Bi, X., Wu, J., Liang, D., Zhang, Y., Feng, Y., and Hopke, P. K.: Dispersion Normalized PMF Provides Insights into the Significant Changes in Source Contributions to PM2.5 after the COVID-19 Outbreak, Environ. Sci. Technol., 54, 9917-9927, https://doi.org/10.1021/acs.est.0c02776, 2020.

Dunlea, E. J., Herndon, S. C., Nelson, D. D., Volkamer, R. M., San Martini, F., Sheehy, P. M., Zahniser, M. S., Shorter, J. H., Wormhoudt, J. C., Lamb, B. K., Allwine, E. J., Gaffney, J. S., Marley, N. A., Grutter, M., Marquez, C., Blanco, S., Cardenas, B., Retama, A., Villegas, C. R. R., Kolb, C. E., Molina, L. T., and Molina, M. J.: Evaluation of nitrogen dioxide chemiluminescence monitors in a polluted urban environment, Atmos. Chem. Phys., 7, 2691-2704, https://doi.org/10.5194/acp-7-2691-2007, 2007.

Evensen, G.: The Ensemble Kalman Filter for Combined State and Parameter Estimation MONTE CARLO TECHNIQUES FOR DATA ASSIMILATION IN LARGE SYSTEMS, IEEE Control Syst. Mag., 29, 83-104, https://doi.org/10.1109/mcs.2009.932223, 2009.

Fan, H., Zhao, C., Yang, Y., and Yang, X.: Spatio-Temporal Variations of the $PM_{2.5}/PM_{10}$ Ratios and Its Application to Air Pollution Type Classification in China, Front. Environ. Sci., 9, https://doi.org/10.3389/fenvs.2021.692440, 2021.

Feng, S., Jiang, F., Wang, H., Wang, H., Ju, W., Shen, Y., Zheng, Y., Wu, Z., and Ding, A.: NOx Emission Changes Over China During the COVID-19 Epidemic Inferred From Surface NO2 Observations, Geophys. Res. Lett., 47, e2020GL090080, https://doi.org/10.1029/2020gl090080, 2020.

He, T. L., Jones, D. B. A., Miyazaki, K., Bowman, K. W., Jiang, Z., Chen, X., Li, R., Zhang, Y., and Li, K.: Inverse modelling of Chinese NOx emissions using deep learning: integrating in situ observations with a satellite-based chemical reanalysis, Atmos. Chem. Phys., 22, 14059-14074, https://doi.org/10.5194/acp-22-14059-2022, 2022.

Hu, Y., Zang, Z., Ma, X., Li, Y., Liang, Y., You, W., Pan, X., and Li, Z.: Four-dimensional variational assimilation for SO2 emission and its application around the COVID-19 lockdown in the spring 2020 over China, Atmos. Chem. Phys., 22, 13183-13200, https://doi.org/10.5194/acp-22-13183-2022, 2022.

Kaiser, J. W., Heil, A., Andreae, M. O., Benedetti, A., Chubarova, N., Jones, L., Morcrette, J. J., Razinger, M., Schultz, M. G., Suttie, M., and van der Werf, G. R.: Biomass burning emissions estimated with a global fire assimilation system based on observed fire radiative power, Biogeosciences, 9, 527-554, https://doi.org/10.5194/bg-9-527-2012, 2012.

Lamsal, L. N., Martin, R. V., van Donkelaar, A., Steinbacher, M., Celarier, E. A., Bucsela, E., Dunlea, E. J., and Pinto, J. P.: Ground-level nitrogen dioxide concentrations inferred from the satellite-borne Ozone Monitoring Instrument, J. Geophys. Res.-Atmos., 113, https://doi.org/10.1029/2007JD009235, 2008.

Li, B., Fan, J., Han, L., Sun, G., Zhang, D., and Zhang, P.: An Industrial Heat Source Extraction Method: BP Neural Network Using Temperature Feature Template (in Chinese with English abstract), Journal of Geo-Information Science, 24, 533-545, 2022.

Li, M., Zhang, Q., Zheng, B., Tong, D., Lei, Y., Liu, F., Hong, C. P., Kang, S. C., Yan, L., Zhang, Y. X., Bo, Y., Su, H., Cheng, Y. F., and He, K. B.: Persistent growth of anthropogenic non-methane volatile organic compound (NMVOC) emissions in China during 1990-2017: drivers, speciation and ozone formation potential, Atmos. Chem. Phys., 19, 8897-8913, https://doi.org/10.5194/acp-19-8897-2019, 2019.

Li, R., Tao, M. H., Zhang, M. G., Chen, L. F., Wang, L. L., Wang, Y., He, X. J., Wei, L. F., Mei, X., and Wang, J.: Application Potential of Satellite Thermal Anomaly Products in Updating Industrial Emission Inventory of China, Geophys. Res. Lett., 48, 7, https://doi.org/10.1029/2021gl092997, 2021.

Ma, C. Q., Wang, T. J., Mizzi, A. P., Anderson, J. L., Zhuang, B. L., Xie, M., and Wu, R. S.: Multiconstituent Data Assimilation With WRF-Chem/DART: Potential for Adjusting Anthropogenic Emissions and Improving Air Quality Forecasts Over Eastern China, J. Geophys. Res.-Atmos., 124, 7393-7412, https://doi.org/10.1029/2019jd030421, 2019.

Ma, T., Duan, F. K., Ma, Y. L., Zhang, Q. Q., Xu, Y. Z., Li, W. G., Zhu, L. D., and He, K. B.: Unbalanced emission reductions and adverse meteorological conditions facilitate the formation of secondary pollutants during the COVID-19 lockdown in Beijing, Sci. Total Environ., 838, 8, https://doi.org/10.1016/j.scitotenv.2022.155970, 2022.

Miyazaki, K. and Eskes, H.: Constraints on surface NO_x emissions by assimilating satellite observations of multiple species, Geophys. Res. Lett., 40, 4745-4750, https://doi.org/10.1002/grl.50894, 2013.

Miyazaki, K., Eskes, H. J., and Sudo, K.: Global NOx emission estimates derived from an assimilation of OMI tropospheric NO_2 columns, Atmos. Chem. Phys., 12, 2263-2288, https://doi.org/10.5194/acp-12-2263-2012, 2012.

Miyazaki, K., Eskes, H., Sudo, K., Boersma, K. F., Bowman, K., and Kanaya, Y.: Decadal changes in global surface NO_x emissions from multi-constituent satellite data assimilation, Atmos. Chem. Phys., 17, 807-837, https://doi.org/10.5194/acp-17-807-2017, 2017.

Peng, Z., Lei, L. L., Liu, Z. Q., Su, J. N., Ding, A. J., Ban, J. M., Chen, D., Kou, X. X., and Chu, K. K.: The impact of multi-species surface chemical observation assimilation on air quality forecasts in China, Atmos. Chem. Phys., 18, 18, https://doi.org/10.5194/acp-18-17387-2018, 2018.

Skachko, S., Errera, Q., Ménard, R., Christophe, Y., and Chabrillat, S.: Comparison of the ensemble Kalman filter and 4D-Var assimilation methods using a stratospheric tracer transport model, Geosci. Model Dev., 7, 1451-1465, https://doi.org/10.5194/gmd-7-1451-2014, 2014.

Streets, D. G., Canty, T., Carmichael, G. R., de Foy, B., Dickerson, R. R., Duncan, B. N., Edwards, D. P., Haynes, J. A., Henze, D. K., Houyoux, M. R., Jacob, D. J., Krotkov, N. A., Lamsal, L. N., Liu, Y., Lu, Z., Martin, R. V., Pfister, G. G., Pinder, R. W., Salawitch, R. J., and Wecht, K. J.: Emissions estimation from satellite retrievals: A review of current capability, Atmos. Environ., 77, 1011-1042, https://doi.org/10.1016/j.atmosenv.2013.05.051, 2013.

Wang, Y. Q., Zhang, X. Y., Sun, J. Y., Zhang, X. C., Che, H. Z., and Li, Y.: Spatial and temporal variations of the concentrations of PM_{10}, $PM_{2.5}$ and PM_1 in China, Atmos. Chem. Phys., 15, 13585-13598, https://doi.org/10.5194/acp-15-13585-2015, 2015.

Zhang, Q., Pan, Y., He, Y., Walters, W. W., Ni, Q., Liu, X., Xu, G., Shao, J., and Jiang, C.: Substantial nitrogen oxides emission reduction from China due to COVID-19 and its impact on surface ozone and aerosol pollution, Sci. Total Environ., 753, 142238, https://doi.org/10.1016/j.scitotenv.2020.142238, 2021.

Zhang, R. X., Zhang, Y. Z., Lin, H. P., Feng, X., Fu, T. M., and Wang, Y. H.: NOx Emission Reduction and Recovery during COVID-19 in East China, Atmosphere, 11, 15, https://doi.org/10.3390/atmos11040433, 2020.

Zuo, P. J., Zong, Z., Zheng, B., Bi, J. Z., Zhang, Q. H., Li, W., Zhang, J. W., Yang, X. Z., Chen, Z. G., Yang, H., Lu, D. W., Zhang, Q. H., Liu, Q., and Jiang, G. B.: New Insights into Unexpected Severe PM2.5 Pollution during the SARS and COVID-19 Pandemic Periods in Beijing, Environ. Sci. Technol., 56, 155-164, https://doi.org/10.1021/acs.est.1c05383, 2022.